CONCEPTUAL DESIGN AND DIMENSIONAL SYNTHESIS OF A NOVEL PARALLEL MECHANISM FOR LOWER-LIMB REHABILITATION

Xinyin Jia, Jianming Che, Haitao Liu, Kun Xiong, Tian Huang
Key Laboratory of Mechanism Theory and Equipment Design of State Ministry of Education, Tianjin University, Tianjin 300072, China
E-mail: liuht@tju.edu.cn

ABSTRACT

This paper introduces a novel 2R1T parallel manipulator redundantly actuated by pneumatic muscles for lower-limb rehabilitation. First, the conceptual design of the proposed 3-DOF parallel mechanism is presented. Then, the inverse kinematics and the generalized Jacobian analysis are carried out. Based on the generalized Jacobian and the constraint characteristics of the mechanism, the force/motion transmissibility of the redundantly actuated parallel mechanism is investigated *via* four individual cases without actuation redundancy, leading to a suitable local transmission index for the evaluation of kinematic performance of the proposed mechanism. Finally, the design variables are optimized by maximizing the mean value of the local transmission index with the aid of genetic algorithm. The numerical result shows that the proposed parallel mechanism can achieve good kinematic performance in its task workspace.

Keywords: conceptual design; kinematic optimization; parallel mechanism; lower-limb rehabilitation.

DESIGN CONCEPTUEL ET SYNTHÈSE DIMENSIONNELLE D'UN NOUVEAU MÉCANISME PARALLÈLE POUR LA RÉHABILITATION DE MINEURS INFÉRIEURS

RÉSUMÉ

Cet article introduit un nouveau manipulateur parallèle 2R1T redondamment actionné par des muscles pneumatiques pour la réhabilitation des membres inférieurs. Tout d'abord, la conception du mécanisme parallèle 3-DOF proposé est présentée. Ensuite, les analyses cinématique inverse et les analyses Jacobiennes généralisées sont réalisées. Sur la base des caractéristiques jacobiennes généralisées et des caractéristiques de contrainte du mécanisme, la transmissibilité force / mouvement du mécanisme parallèle à action redondante est étudiée par quatre cas individuels sans redondance d'actionnement, conduisant à un indice de transmission local approprié pour l'évaluation de la performance cinématique du mécanisme proposé mécanisme. Enfin, les variables de conception sont optimisées en maximisant la valeur moyenne de l'indice de transmission local à l'aide d'un algorithme génétique. Le résultat numérique montre que le mécanisme parallèle proposé permet d'obtenir de bonnes performances cinématiques dans son espace de travail.

Mots-clés : design conceptuel; optimisation cinématique; mécanisme parallèle; rééducation des membres inférieurs.

1 INTRODUCTION

Stroke is the primary cause of permanent disability and one of the leading reasons of death worldwide. Survivors after stroke may experience paralysis or hemiparesis that reduce the mobile capabilities of lower limbs, resulting in the difficulty in performing activities of daily living [1]. It has been proven that repetitive and intensive rehabilitation training is helpful and effective to regain the walking ability [2]. Traditional lower-limb rehabilitation needs two or three therapists to manually assist the patient to move the legs and stabilize the patient's posture [3]. Due to the heavy burden of labor and healthcare costs, there is a high demand for building robotized system as an alternative to therapists to implement rehabilitation treatments.

Over the last two decades, different kinds of robotic systems for lower-limb rehabilitation have been developed, which can be roughly classified into two groups: exoskeleton gait trainers [4,5,6] and foot-plate-based gait trainers [7,8,9]. The exoskeleton gait trainer can be considered as a powered leg orthosis with actuators at the hip and knee joints, while the gait pattern is achieved by controlling angular position of the joints' trajectories. Usually, it is additionally combined with a body weight support system and a treadmill. Typical examples of this kind of robotic systems are Lokomat [4], LokoHelp [5], and ReoAmbulator [6]. In contrast, another idea for lower-limb rehabilitation is to realize the gait training by distally guiding the movements of foot, resulting in foot-plate-based gait trainers. Since no treadmill is included in the system, the training is not restricted to walking on level ground. In other words, different gait patterns can be simulated such as climbing stairs and walking on slopes. GaitTrainer [7], HapticWalker [8], and GaitMaster5 [9] exemplify the success of such systems. One advantage of foot-plate-based gait trainers is that the knees are not fixed, such that therapists can physically correct the knee movement, if necessary [3].

In order to meet the requirements of moving capability, parallel mechanisms have been employed in foot-plate-based gait trainers [10,11]. As a preliminary to the design of a parallel mechanism, the kinematic optimization attracts lots of attentions [12,13]. The algebraic characteristics of the Jacobian matrix [14], such as condition number, singular values, and determinant, are the most widely used kinematic performance indices. However, due to the inconsistency in the physical units of the Jacobian, these indices cannot be directly adopted for kinematic performance evaluation of parallel mechanisms having coupled translations and rotations [15]. One way to overcome this problem is to formulate a dimensionally homogeneous Jacobian in which all entries have the same physical units [16,17]. This way is only suitable for those parallel mechanisms actuated by the same type of joints, either prismatic or revolute joints. An alternative way to circumvent inhomogeneity of coordinates is based on the notion of virtual coefficient representing the virtual power done by a unit wrench on a unit twist [18]. Great efforts have been made towards analyzing the motion/force transmissibility of parallel mechanisms. The virtual coefficient between the transmission wrench screw (TWS) and output twist screw (OTS) was defined as a transmission factor (TF) in [19]. To normalize the transmission factor, the transmission index only depending on the geometric properties of the mechanisms was proposed in [20]. A generalized transmission index for spatial linkages was presented in [21]. And several indices for parallel mechanisms, such as the input transmission index (ITI), the output transmission index (OTI), and the constraint transmission index (CTI) [22], were defined to measure the closeness between a pose and a singular configuration. Recently, a new approach to determine the maximal virtual coefficient of parallel mechanisms was proposed by taking into account both the TWS and OTS axis-orientation variations [23]. Furthermore, the indices indicating the minimal motion/force transmission for parallel mechanisms with actuation and kinematic redundancy were proposed in [24].

In this paper, the kinematic optimization of a novel 2R1T parallel mechanism [25] actuated by pneumatic muscles for lower-limb rehabilitation is presented. The rest of the paper is organized as follows. Section 2 introduces the conceptual design of the 2R1T parallel mechanism. The inverse kinematics is investigated in section 3. Then the generalized Jacobian analysis is carried out in section 4, followed by the investigation of motion/force transmissibility of the parallel mechanism. The kinematic

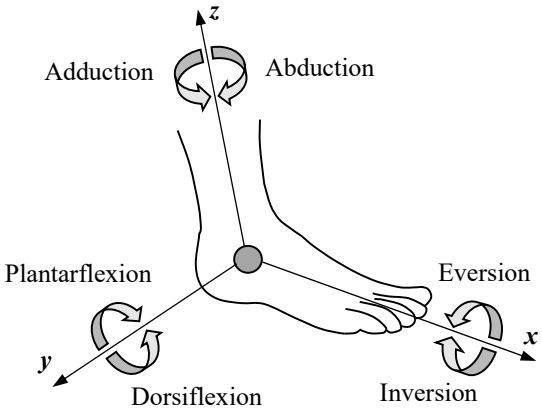

Fig. 1. Movements of human ankle.

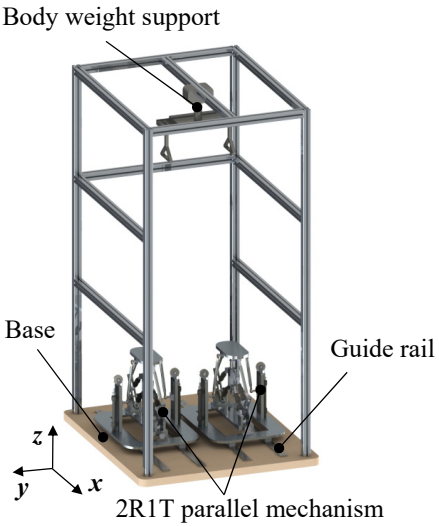

Fig. 2. Lower-limb rehabilitation robot.

optimization is studied in Section 6 by using the genetic algorithm to obtain a set of optimized design variables, before conclusions are drawn in section 7.

2 CONCEPTUAL DESIGN

First of all, the movements of human ankle and their ranges are analyzed as a prerequisite for the design of a parallel mechanism for lower-limb rehabilitation. As shown in Fig. 1, the ankle motion can be described by three different rotations, i.e. inversion/eversion, plantarflexion/dorsiflexion, and abduction/adduction. However, only the first two movements are dominant actions in lower-limb rehabilitation. Besides, the motion of lifting the foot off the ground, i.e. a translation along the *z*-axis, should also be taken into account. According to [26], the ranges of inversion/eversion and plantar flexion/dorsiflexion are [-20°, 20°] and [-40°, 40°], respectively, while the range of translation is [0 mm, 200 mm].

Fig. 2 shows the lower-limb rehabilitation robot, which is composed of two 2R1T parallel

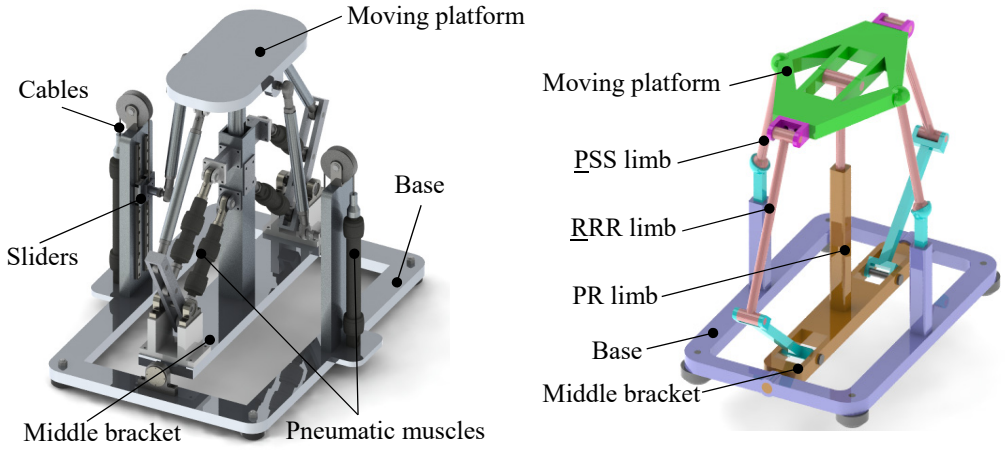

(a) (b)

Fig.3 CAD model (a) and structural sketch (b) of the 2R1T parallel mechanism

mechanisms, a body weight support system, guide rails, and a base. The 3D model and structural sketch of the proposed 3-DOF parallel mechanism is shown in Fig. 3, where the pneumatic muscles are employed as actuators. Its topological structure is a 2-PSS-R(2-RRR-PR) parallel mechanism. Here, R, P, and S denote revolute, prismatic, and spherical joints, respectively; while P and R denote actuated prismatic and revolute joints. A critical feature is that the mechanism comprises two actuated PSS limbs plus a stand-along 2-DOF planar parallel mechanism containing two actuated RRR limbs and a properly constrained passive PR limb, connected by a pair of R joints to the base at either side of the middle bracket (see Fig. 3(b)). Then, manipulated by pneumatic muscles, the moving platform undergoes one translation along the direction of the P joint, and two rotations about the axes of the R joint of PR limb and the R joint connecting the middle bracket to the base, respectively. Consequently, by providing an additional translation along the direction of x-axis to the base of the parallel mechanism, the rehabilitation robot can separately control the length and height of steps and the rotational angle of foot.

3 INVERSE KINEMATICS

Fig. 4(a) shows the schematic diagram of the proposed parallel mechanism. Let B_i, P_i and A_i ($i=1,3$) denote the centers of the revolute joints of the RRR limb (see Fig. 4); B_i, P_i, and A_i ($i=2,4$) denote the intersection of prismatic joint and the base, and the centers of spherical joints of the PSS limb, respectively. A global frame $\mathcal{K}$ is attached to the center point O of the base with the z-axis normal to the base, the x-axis pointing towards point B_1, and the y-axis satisfying the right-hand rule. Similarly, a local frame $\mathcal{K}'$ is attached to the center point O' of the moving platform with the w-axis normal to the platform, u-axis pointing towards joint A_1, and the v-axis satisfying the right-hand rule. Consequently, the orientation matrix of $\mathcal{K}'$ with respect to $\mathcal{K}$ can be expressed by

$$\boldsymbol{R}=\boldsymbol{R}_x\boldsymbol{R}_v=\begin{bmatrix}\boldsymbol{u} & \boldsymbol{v} & \boldsymbol{w}\end{bmatrix}=\begin{bmatrix}\cos\theta & 0 & \sin\theta\\ \sin\psi\sin\theta & \cos\psi & -\sin\psi\cos\theta\\ -\cos\psi\sin\theta & \sin\psi & \cos\psi\cos\theta\end{bmatrix} \tag{1}$$

where $\boldsymbol{u}$, $\boldsymbol{v}$, and $\boldsymbol{w}$ are the unit vectors of u-, v-, and w-axis, respectively.

Note that the PR limb and two RRR limbs constitute a planar mechanism as shown in Fig. 4(b). The

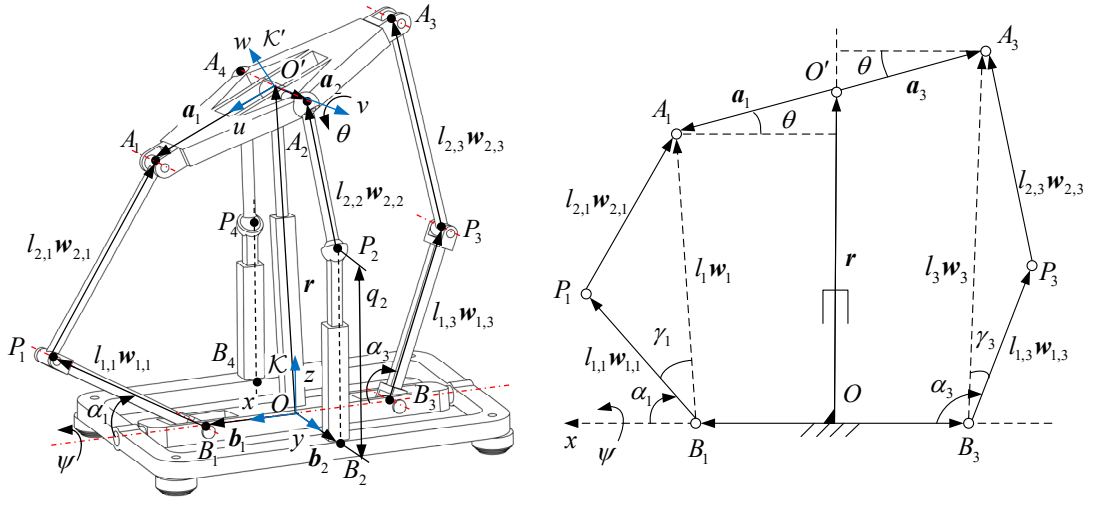

Fig. 4. Schematic diagram of the 2R1T parallel mechanism (a) and the planar mechanism (b).

following close-loop equations can be derived.

$$\begin{cases} \boldsymbol{r} = \boldsymbol{b}_i + l_i \boldsymbol{w}_i - \boldsymbol{a}_i \\ l_i \boldsymbol{w}_i = l_{1,i} \boldsymbol{w}_{1,i} + l_{2,i} \boldsymbol{w}_{2,i} \end{cases}, \ i = 1, 3 \tag{2}$$

$$\boldsymbol{r} = \boldsymbol{b}_i + q_i \boldsymbol{z} + l_{2,i} \boldsymbol{w}_{2,i} - \boldsymbol{a}_i, \ i = 2, 4 \tag{3}$$

$$\boldsymbol{b}_i = b_i \begin{pmatrix} \cos\beta_i & \sin\beta_i & 0 \end{pmatrix}^{\mathrm{T}}, \ \boldsymbol{a}_i = \boldsymbol{R}\boldsymbol{a}_{i0}, \ \boldsymbol{a}_{i0} = a_i \begin{pmatrix} \cos\beta_i & \sin\beta_i & 0 \end{pmatrix}^{\mathrm{T}}, \ \beta_i = (i-1)\pi/2,$$
$$\boldsymbol{r} = r(0 \ -\sin\psi \ \cos\psi)^{\mathrm{T}}$$

where $\boldsymbol{b}_i$ is position vector of point B_i evaluated in $\mathcal{K}$; $\boldsymbol{a}_{i0}$ is the position vector of point A_i evaluated in $\mathcal{K}'$; $l_{1,i}\boldsymbol{w}_{1,i} = \overline{B_i P_i}$, $l_{2,i}\boldsymbol{w}_{2,i} = \overline{P_i A_i}$, $l_i \boldsymbol{w}_i = \overline{B_i A_i}$, and $\boldsymbol{r} = \overline{OO'}$. From the Eq. (2) and Eq. (3), we can obtain

$$\begin{cases} l_i = \left\| \boldsymbol{r} - \boldsymbol{b}_i + \boldsymbol{a}_i \right\| \\ \boldsymbol{w}_i = \left(\boldsymbol{r} - \boldsymbol{b}_i + \boldsymbol{a}_i \right) / l_i \end{cases}, \ i = 1, 3 \tag{4}$$

$$\begin{cases} q_i = c_{z,i} - \sqrt{l_{2,i}^2 - c_{x,i}^2 - c_{y,i}^2} \\ \boldsymbol{w}_{2,i} = \left(\boldsymbol{r} - \boldsymbol{b}_i - q_i \boldsymbol{z} + \boldsymbol{a}_i \right) / l_{2,i} \end{cases}, \ i = 2, 4 \tag{5}$$

$$c_{x,i} = \boldsymbol{a}_i^{\mathrm{T}} \boldsymbol{x}, \ c_{y,i} = \left(\boldsymbol{a}_i - \boldsymbol{b}_i \right)^{\mathrm{T}} \boldsymbol{y} - r\sin\psi, \ c_{z,i} = \boldsymbol{a}_i^{\mathrm{T}} \boldsymbol{z} + r\cos\psi$$

where $\boldsymbol{x}$, $\boldsymbol{y}$, and $\boldsymbol{z}$ are the unit vectors of *x*-, *y*-, and *z*-axis, respectively. Note that the following equation holds in $\triangle A_i P_i B_i$

$$\gamma_i = \arccos\left(\frac{{l_{1,i}}^2 + l_i^2 - {l_{2,i}}^2}{2 l_{1,i} l_i} \right), \ i = 1, 3 \tag{6}$$

then α_i can be solved by

$$\begin{cases} \alpha_i = \arccos\left(\boldsymbol{x}^{\mathrm{T}} \boldsymbol{w}_i \right) + (i-2)\gamma_i \\ \boldsymbol{w}_{1,i} = \boldsymbol{R}_x \boldsymbol{w}_{10,i} \\ \boldsymbol{w}_{2,i} = \left(l_i \boldsymbol{w}_i - l_{1,i} \boldsymbol{w}_{1,i} \right) / l_{2,i} \end{cases}, \ i = 1, 3 \tag{7}$$

where $\boldsymbol{w}_{10,i} = \begin{pmatrix} \cos\alpha_i & \sin\alpha_i & 0 \end{pmatrix}^{\mathrm{T}}$. Hence, given the position vector $\boldsymbol{r}$ and two rotational angles ψ and θ, the input joint variables α_i ($i = 1, 3$) and q_i ($i = 2, 4$) can be evaluated using Eq. (5) and Eq. (7). Furthermore, in order to ensure that $\overline{B_i P_i}$, $\overline{P_i A_i}$, and $\overline{B_i A_i}$ could form a triangle, additional constraint equations can be derived.

$$\begin{cases} \left| l_{2,i} - l_{1,i} \right| < l_i < \left| l_{2,i} + l_{1,i} \right| \\ l_i^2 = \left(b_i - a_i \cos\theta \right)^2 + \left(r + (i-2) a_i \sin\theta \right)^2 \end{cases}, \ i = 1, 3 \tag{8}$$

From the Eq. (8), the constraint condition of r in the task workspace can be achieved.

$$\max\left\{ r_0(\theta) \right\} < r < \min\left\{ r_1(\theta) \right\}, \ i = 1, 3 \tag{9}$$

where

$$r_0(\theta)=\sqrt{\left(l_{2,i}-l_{1,i}\right)^2-\left(b_i-a_i\cos\theta\right)^2}+\left(i-2\right)a_i\sin\theta$$

$$r_1(\theta)=\sqrt{\left(l_{2,i}+l_{1,i}\right)^2-\left(b_i-a_i\cos\theta\right)^2}+\left(i-2\right)a_i\sin\theta$$

$$\left|l_{2,i}-l_{1,i}\right|>\left|b_i-a_i\cos\theta\right|$$

Moreover, from Eq. (3) it can be found that since $\boldsymbol{r}$, $\boldsymbol{b}_i$, $\boldsymbol{z}$, and $\boldsymbol{a}_i$ are perpendicular to x-axis, $\boldsymbol{w}_{2,i}$ should be perpendicular to the same axis.

4 GENERALIZED JACOBIAN ANALYSIS

For convenience, attach an instantaneous frame $\mathcal{K}_0$ at point O' with its three orthogonal axes parallel to those of frame $\mathcal{K}$. The coordinates of all screws are evaluated in $\mathcal{K}_0$ unless stated otherwise. Then, the unit wrenches of actuations and constraints provided by limb 1 and limb 3 can be obtained [27, 28]

$$\hat{\$}_{wa,1,i}=\begin{pmatrix}\boldsymbol{w}_{2,i}\\ \boldsymbol{a}_i\times\boldsymbol{w}_{2,i}\end{pmatrix},\ \hat{\$}_{wc,1,i}=\begin{pmatrix}\boldsymbol{v}\\ -\boldsymbol{r}\times\boldsymbol{v}\end{pmatrix},\ \hat{\$}_{wc,2,i}=\begin{pmatrix}\boldsymbol{0}\\ \boldsymbol{x}\times\boldsymbol{v}\end{pmatrix},\ i=1,3 \tag{10}$$

while the unit wrenches of actuations provided by limb 2 and limb 4 are

$$\hat{\$}_{wa,1,i}=\begin{pmatrix}\boldsymbol{w}_{2,i}\\ \boldsymbol{a}_i\times\boldsymbol{w}_{2,i}\end{pmatrix},\ i=2,4 \tag{11}$$

Since the RPR limb is a 3-DOF passive limb, its unit wrenches of constraints can be given as

$$\hat{\$}_{wc,1,5}=\begin{pmatrix}\boldsymbol{x}\\ \boldsymbol{0}\end{pmatrix},\ \hat{\$}_{wc,2,5}=\begin{pmatrix}\boldsymbol{v}\\ -\boldsymbol{r}\times\boldsymbol{v}\end{pmatrix},\ \hat{\$}_{wc,3,5}=\begin{pmatrix}\boldsymbol{0}\\ \boldsymbol{x}\times\boldsymbol{v}\end{pmatrix} \tag{12}$$

From Eq. (10) and Eq. (12), it can be seen that $\hat{\$}_{wc,1,i}=\hat{\$}_{wc,2,5}$ and $\hat{\$}_{wc,2,i}=\hat{\$}_{wc,3,5}$ ($i=1,3$), which are the common constraints of the 2-RRR-PR planar parallel mechanism. Therefore, the constraint wrenches imposed on the moving platform can be considered to be provided only by the RPR limb. Due to that, if any one of the active limb is removed from the parallel mechanism, the mobility of the moving platform retains the same. Consequently, the linear map between the twist $\$_t$ of the moving platform and the joint variations can be formulated as [27, 29]

$$\boldsymbol{J}\$_t=\boldsymbol{\Lambda}\boldsymbol{\rho}_t \tag{13}$$

$$\boldsymbol{J}=\boldsymbol{W}^{\mathrm{T}},\ \boldsymbol{W}=\begin{bmatrix}\boldsymbol{W}_a & \boldsymbol{W}_c\end{bmatrix},\ \boldsymbol{W}_a=\begin{bmatrix}\hat{\$}_{wa,1,1} & \hat{\$}_{wa,1,2} & \hat{\$}_{wa,1,3} & \hat{\$}_{wa,1,4}\end{bmatrix},\ \boldsymbol{W}_c=\begin{bmatrix}\hat{\$}_{wc,1,5} & \hat{\$}_{wc,2,5} & \hat{\$}_{wc,3,5}\end{bmatrix}$$

$$\boldsymbol{\Lambda}=\boldsymbol{\Lambda}_a=\mathrm{diag}\begin{bmatrix}\boldsymbol{\Lambda}_a & \boldsymbol{\Lambda}_c\end{bmatrix},\ \boldsymbol{\Lambda}_a=\mathrm{diag}\left[\hat{\$}_{wa,1,i}^{\mathrm{T}}\hat{\$}_{ta,1,i}\right],\ \boldsymbol{\Lambda}_c=\mathrm{diag}\left[\hat{\$}_{wc,j,5}^{\mathrm{T}}\hat{\$}_{tc,j,5}\right]$$

$$\hat{\$}_{ta,1,i}=\begin{cases}\left(\left(\left(\boldsymbol{a}_i-l_{2,i}\boldsymbol{w}_{2,i}-l_{1,i}\boldsymbol{w}_{1,i}\right)\times\boldsymbol{v}\right)^{\mathrm{T}}\ \ \boldsymbol{v}^{\mathrm{T}}\right)^{\mathrm{T}} & i=1,3\\ \left(\boldsymbol{z}^{\mathrm{T}}\ \ 0\right)^{\mathrm{T}} & i=2,4\end{cases}$$

$$\boldsymbol{\rho}_t=\left(\boldsymbol{\rho}_{ta}^{\mathrm{T}}\ \ \boldsymbol{\rho}_{tc}^{\mathrm{T}}\right)^{\mathrm{T}},\ \boldsymbol{\rho}_{ta}=\left(\rho_{ta,1,1}\ \ \rho_{ta,1,2}\ \ \rho_{ta,1,3}\ \ \rho_{ta,1,4}\right)^{\mathrm{T}},\ \boldsymbol{\rho}_{tc}=\left(\rho_{tc,1,5}\ \ \rho_{tc,2,5}\ \ \rho_{tc,3,5}\right)^{\mathrm{T}}$$

where $\boldsymbol{J}$ is known as generalized Jacobian [27]; $\rho_{ta,1,i}$ and $\hat{\$}_{ta,1,i}$ are the amplitude and unit screw of limb i ($i=1,2,3,4$); $\rho_{tc,j,5}$ and $\hat{\$}_{tc,j,5}$ are the amplitude and unit screw of the jth ($j=1,2,3$) twist of restrictions of the RPR limb. According to [30], $\boldsymbol{\Lambda}_c=\boldsymbol{I}_3$ where $\boldsymbol{I}_3$ is an identity matrix of order three. Especially, in velocity analysis, $\$_t$, $\boldsymbol{\rho}_{ta}$, and $\boldsymbol{\rho}_{tc}$ in Eq. (13) turn into

$$\$_t=\begin{pmatrix}\dot{\boldsymbol{r}}\\ \boldsymbol{\omega}\end{pmatrix},\ \dot{\boldsymbol{\rho}}=\begin{pmatrix}\dot{\boldsymbol{q}}\\ \boldsymbol{0}\end{pmatrix},\ \dot{\boldsymbol{q}}=\begin{pmatrix}\dot{\alpha}_1 & \dot{q}_2 & \dot{\alpha}_3 & \dot{q}_4\end{pmatrix}^{\mathrm{T}},\ \boldsymbol{\rho}_{tc}=\boldsymbol{0} \tag{14}$$

where $\dot{\boldsymbol{r}}$ and $\boldsymbol{\omega}$ are the linear velocity of point O' and the angular velocity of the platform, respectively.

5 TRANSMISSIBILITY ANALYSIS

Based on the generalized Jacobian analysis, three kinds of transmission indices defined in [22], i.e. the input transmission index, the output transmission index, and the constraint transmission index, are employed to investigate the force/motion transmissibility of the 2R1T parallel mechanism. It has to be pointed out that since the proposed parallel mechanism is redundantly actuated, these transmission indices cannot be used directly. However, due to the characteristics of the common constraints, a non-redundantly actuated 3-DOF parallel mechanism can be achieved by removing any one of the active limbs from the 2R1T parallel mechanism. Therefore, the force/motion transmissibility analysis can be individually investigated for four cases as shown in Fig. 5 and summarized in Table 1. Without losing generality, we take Case 1 as an example to give a brief review of the definitions of these three transmission indices. Similar analysis can be carried out for the other three cases.

A simplified 3D model of Case 1 is shown in Fig. 5(a), where limb 4 is removed. Hence, the basis of the wrench space [29] can be expressed by

$$\boldsymbol{W}_1=\begin{bmatrix}\boldsymbol{W}_{a,1} & \boldsymbol{W}_c\end{bmatrix} \tag{15}$$

$$\boldsymbol{W}_{a,1}=\begin{bmatrix}\hat{\$}_{wa,1,1} & \hat{\$}_{wa,1,2} & \hat{\$}_{wa,1,3}\end{bmatrix},\ \boldsymbol{W}_c=\begin{bmatrix}\hat{\$}_{wc,1,5} & \hat{\$}_{wc,2,5} & \hat{\$}_{wc,3,5}\end{bmatrix}$$

Since the twist $\$_t$ of the moving platform keeps unchanged, for any singularity-free configuration, Eq. (13) can be reformulated as

$$\$_t=\boldsymbol{W}_1^{-\mathrm{T}}\boldsymbol{\Lambda}_1\boldsymbol{\rho}_{t,1} \tag{16}$$

$$\boldsymbol{\rho}_{t,1}=\begin{pmatrix}\boldsymbol{\rho}_{ta,1}^{\mathrm{T}} & \boldsymbol{\rho}_{tc}^{\mathrm{T}}\end{pmatrix}^{\mathrm{T}},\ \boldsymbol{\rho}_{ta,1}=\begin{pmatrix}\rho_{ta,1,1} & \rho_{ta,1,2} & \rho_{ta,1,3}\end{pmatrix}^{\mathrm{T}},\ \boldsymbol{\Lambda}_1=\begin{bmatrix}\boldsymbol{\Lambda}_{a,1} & \\ & \boldsymbol{\Lambda}_c\end{bmatrix},\ \boldsymbol{\Lambda}_{a,1}=\mathrm{diag}\left[\hat{\$}_{wa,1,i}^{\mathrm{T}}\hat{\$}_{ta,1,i}\right],\ i=1,2,3$$

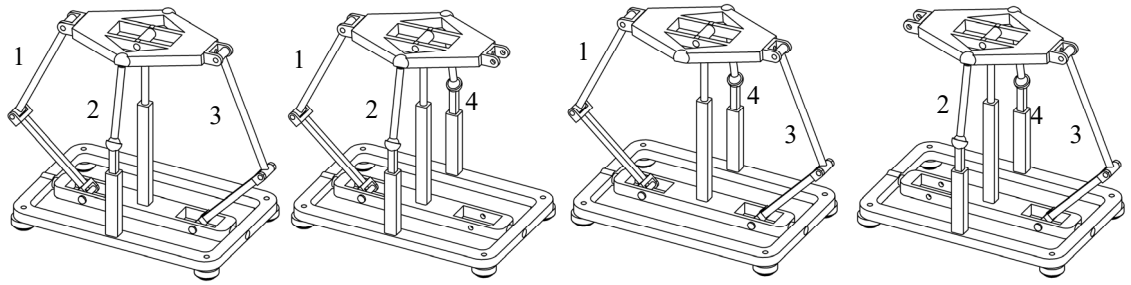

(a) Case 1 (b) Case 2 (c) Case 3 (d) Case 4

Fig. 5. Simplified 3D models of four cases.

Table 1. Wrench systems of four cases.

Case	limb removed	$\boldsymbol{W}_a$	$\boldsymbol{W}_c$
1 (Fig. 5(a))	limb 4	$\begin{bmatrix} \boldsymbol{w}_{2,1} & \boldsymbol{w}_{2,2} & \boldsymbol{w}_{2,3} \\ \boldsymbol{a}_1 \times \boldsymbol{w}_{2,1} & \boldsymbol{a}_2 \times \boldsymbol{w}_{2,2} & \boldsymbol{a}_3 \times \boldsymbol{w}_{2,3} \end{bmatrix}$	$\begin{bmatrix} \boldsymbol{x} & \boldsymbol{v} & \boldsymbol{0} \\ \boldsymbol{0} & -\boldsymbol{r} \times \boldsymbol{v} & \boldsymbol{x} \times \boldsymbol{v} \end{bmatrix}$
2 (Fig. 5(b))	limb 3	$\begin{bmatrix} \boldsymbol{w}_{2,1} & \boldsymbol{w}_{2,2} & \boldsymbol{w}_{2,4} \\ \boldsymbol{a}_1 \times \boldsymbol{w}_{2,1} & \boldsymbol{a}_2 \times \boldsymbol{w}_{2,2} & \boldsymbol{a}_4 \times \boldsymbol{w}_{2,4} \end{bmatrix}$	
3 (Fig. 5(c))	limb 2	$\begin{bmatrix} \boldsymbol{w}_{2,1} & \boldsymbol{w}_{2,3} & \boldsymbol{w}_{2,4} \\ \boldsymbol{a}_1 \times \boldsymbol{w}_{2,1} & \boldsymbol{a}_3 \times \boldsymbol{w}_{2,3} & \boldsymbol{a}_4 \times \boldsymbol{w}_{2,4} \end{bmatrix}$	
4 (Fig. 5(d))	limb 1	$\begin{bmatrix} \boldsymbol{w}_{2,2} & \boldsymbol{w}_{2,3} & \boldsymbol{w}_{2,4} \\ \boldsymbol{a}_2 \times \boldsymbol{w}_{2,2} & \boldsymbol{a}_3 \times \boldsymbol{w}_{2,3} & \boldsymbol{a}_4 \times \boldsymbol{w}_{2,4} \end{bmatrix}$	

Then, $\$_t$ can be expressed by a new set of basis of the twist space.

$$\$_t = \boldsymbol{T}_1^* \boldsymbol{\rho}_{t,1}^*, \ \boldsymbol{\rho}_{t,1}^* = \boldsymbol{\Lambda}_1^{*-1} \boldsymbol{\Lambda}_1 \boldsymbol{\rho}_{t,1} \tag{17}$$

$$\boldsymbol{T}_1^* = \begin{bmatrix} \boldsymbol{T}_{a,1}^* & \boldsymbol{T}_{c,1}^* \end{bmatrix}, \ \boldsymbol{T}_{a,1}^* = \begin{bmatrix} \hat{\$}_{ta,1,1}^* & \hat{\$}_{ta,1,2}^* & \hat{\$}_{ta,1,3}^* \end{bmatrix}, \ \boldsymbol{T}_{c,1}^* = \begin{bmatrix} \hat{\$}_{tc,1,5}^* & \hat{\$}_{tc,2,5}^* & \hat{\$}_{tc,3,5}^* \end{bmatrix}$$

where $\boldsymbol{T}_1^*$ is obtained by first computing $\overline{\boldsymbol{T}}_1^* = \boldsymbol{W}_1^{-\mathrm{T}}$ and then normalizing the columns in $\overline{\boldsymbol{T}}_1^*$ as unit twists by extracting the reciprocals of the magnitudes into a diagonal matrix $\boldsymbol{\Lambda}_1^*$ such that $\overline{\boldsymbol{T}}_1^* = \boldsymbol{W}_1^{-\mathrm{T}} \boldsymbol{\Lambda}_1^*$. Consequently, the input transmission index $k_{I,1}$, the output transmission index $k_{O,1}$ and the constraint transmission index $k_{C,1}$ for Case 1 can be defined as follows [22]

$$\textbf{ITI} \quad k_{I,1} = \min_i \left\{ \frac{\left| \hat{\$}_{wa,1,i} \circ \hat{\$}_{ta,1,i} \right|}{\left| \hat{\$}_{wa,1,i} \circ \hat{\$}_{ta,1,i} \right|_{\max}} \right\}, \ i = 1,2,3 \tag{18}$$

$$\textbf{OTI} \quad k_{O,1} = \min_i \left\{ \frac{\left| \hat{\$}_{wa,1,i}^{\mathrm{T}} \circ \hat{\$}_{ta,1,i}^* \right|}{\left| \hat{\$}_{wa,1,i}^{\mathrm{T}} \circ \hat{\$}_{ta,1,i}^* \right|_{\max}} \right\}, \ i = 1,2,3 \tag{19}$$

$$\textbf{CTI} \quad k_{C,1} = \min_j \left\{ \frac{\left| \hat{\$}_{wc,j,5}^{\mathrm{T}} \circ \hat{\$}_{tc,j,5}^* \right|}{\left| \hat{\$}_{wc,j,5}^{\mathrm{T}} \circ \hat{\$}_{tc,j,5}^* \right|_{\max}} \right\}, \ j = 1,2,3 \tag{20}$$

where $\left| \square \right|_{\max}$ is the local maximum of a virtual coefficient that is computed utilizing the method proposed in [23]. Note that these three transmission indices describe the closeness to three types of singularities of the mechanism [22], and if the value of any of them equals zero, the singularity will occur. Hence, the transmission indices should be as large as possible so as to obtain a good kinematic performance. Therefore, a local transmission index is defined as

$$k_1 = k_{I,1} k_{O,1} k_{C,1} \tag{21}$$

Obviously, the larger the value of k_1, the better the force/motion transmissibility at a local configuration. Analogously, the local transmission indices k_2, k_3, and k_4 for the other three cases can be

defined in a similar way. Since k_χ ($\chi = 1,2,3,4$) is dependent upon $\boldsymbol{W}_\chi$, if none of them is fully ranked, the singularity will occur. Therefore, a local performance index to identify the singularity of the 2R1T parallel mechanism can be defined by

$$k = \max\{k_1 \quad k_2 \quad k_3 \quad k_4\} \tag{22}$$

6 KINEMATIC OPTIMIZATION

In order to achieve a symmetrical structure, let $b_1 = b_3$, $a_1 = a_3$, $l_{2,1} = l_{2,3}$, $l_{2,2} = l_{2,4}$, $l_{1,1} = l_{1,3}$, $b_2 = b_4$, and $a_2 = a_4$. There are seven design variables of the 2R1T parallel mechanism. Without losing generality, let a_2, b_1, b_2, $l_{2,1}$, $l_{2,2}$, and $l_{1,1}$ be normalized by a_1 such that

$$\lambda_1 = \frac{a_2}{a_1},\ \lambda_2 = \frac{b_1}{a_1},\ \lambda_3 = \frac{b_2}{a_1},\ \lambda_4 = \frac{l_{2,1}}{a_1},\ \lambda_5 = \frac{l_{2,2}}{a_1},\ \lambda_6 = \frac{l_{1,1}}{a_1} \tag{23}$$

According to [26], the ranges of rotational angles ψ and θ are given as [-20°, 20°] and [-40°, 40°], respectively. Due to Eq. (9), the value of r can be determined by a given set of design variables. Besides, the following limitations of design variables are taken into account.

$$0.5 \le \lambda_1 \le 1,\ 0.5 \le \lambda_2 \le 1.5,\ 2 \le \lambda_3 \le 3,\ 5 \le \lambda_4 \le 6,\ 4 \le \lambda_5 \le 5,\ 1.5 \le \lambda_6 \le 2 \tag{24}$$

Since the k proposed in Eq. (22) is a local transmission index, a global transmission index served as the objective function for optimization is defined

$$\begin{aligned} &\bar{k}(\boldsymbol{X}) = \frac{\int_V k dV}{\int_V dV} \to \max,\ \boldsymbol{X} = (\lambda_1 \quad \lambda_2 \quad \lambda_3 \quad \lambda_4 \quad \lambda_5 \quad \lambda_6)^{\mathrm{T}} \\ &\text{s.t.} \quad \boldsymbol{X}_0 \le \boldsymbol{X} \le \boldsymbol{X}_1 \end{aligned} \tag{25}$$

where V is the volume of W_t that denotes the task workspace of the parallel mechanism, $\boldsymbol{X}_0$ and $\boldsymbol{X}_1$ represents the lower and upper boundaries of the design vector $\boldsymbol{X}$. The geometrical meaning of $\bar{k}(\boldsymbol{X})$ can be interpreted as the mean value of k in W_t. The optimal design of the 2R1T parallel mechanism in this paper is to search for the optimal values of design variables in their domains in order to achieve a largest value of $\bar{k}(\boldsymbol{X})$.

In order to solve the optimization problem, the genetic algorithm (GA) tool-box in MATLAB is employed. Note that the GA tool-box is only valid for minimization, hence a fitness function is defined as follows in order to achieve a value falling into a range of [0, 1].

$$f(\boldsymbol{X}) = 1 - \bar{k}(\boldsymbol{X}) \tag{26}$$

Given the number of design variables and the bounds of solution domain, the evolutionary process is shown in Fig. 6(a). The optimized design variables are given in Table 2, with the aid of which the distribution of k in W_t is illustrated in Fig. 6(b), where different colours denote the variations of k. It can be found that k is symmetrical with respect to θ and ψ, and varies in a range of [0.6, 0.85].

Table 2. Results of optimization.

Design parameters	λ_1	λ_2	λ_3	λ_4	λ_5	λ_6	$\bar{k}$
Optimized design	0.997	1.498	2.941	5.003	4.956	1.582	0.7283

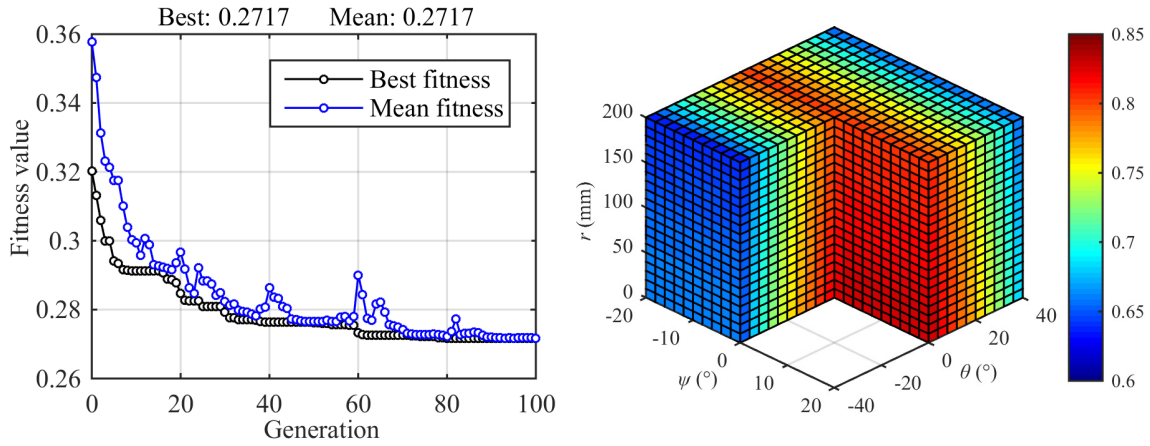

(a) (b)

Fig. 6. Evolutionary process of the optimization (a) and distribution of k in W_t (b).

Moreover, the parallel mechanism achieves better motion/force transmissibility in the central areas of W_t. Numerical result shows that the mean value $\bar{k}$ is 0.7283, indicating that the optimized parallel mechanism has good kinematic performance in W_t. Fig.7 shows the variation of $f(\boldsymbol{X})$ versus the ith ($i=1,2,...,6$) design variable within its range while the rest design variables take the optimized values. It is easy to see that $f(\boldsymbol{X})$ is a monotonically increasing function of λ_4, meaning that better kinematic performance can be achieved at the cost of reducing the length of $l_{2,1}$; meanwhile $f(\boldsymbol{X})$ is a monotonically decreasing function of λ_1, λ_2, λ_3, λ_5, and λ_6, indicating that a set of larger a_2, b_1, b_2, $l_{2,2}$, and $l_{1,1}$ is helpful to improve the kinematic performance. It can also be concluded that λ_2 and λ_6 have little effect on the variation of $f(\boldsymbol{X})$ compared to the rest design variables. Therefore, λ_2 and λ_6 can be excluded from the optimization problem by assigning the upper bounds to these two design variables.

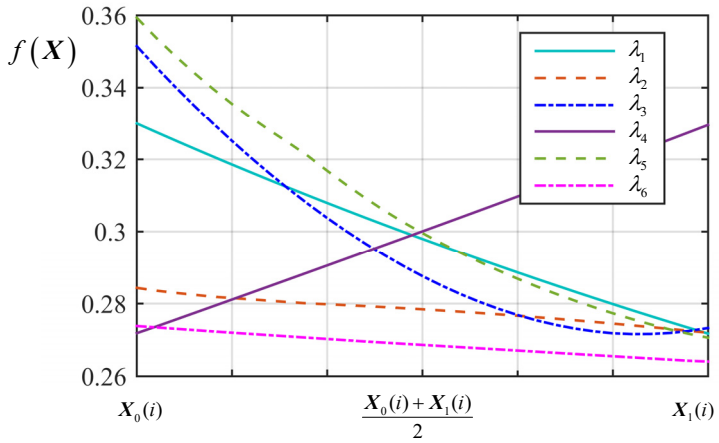

Fig. 7. Variations of $f(\boldsymbol{X})$ vs. design variables

7 CONCLUSION

In this paper, a novel 3-DOF parallel mechanism redundantly actuated by pneumatic muscles for lower-limb rehabilitation is proposed. The mechanism is capable of carrying out the dominant movements required for gait rehabilitation. In addition, due to the employment of pneumatic muscles, it is feasible to apply force control during rehabilitation therapies. Based on the generalized Jacobian analysis, the force/motion transmissibility of the redundantly actuated and overconstrained parallel mechanism is studied *via* four individual cases without actuation redundancy, resulting in the definition of a local transmission index that can be employed as a measure to evaluate the kinematic performance of the proposed mechanism. With the aid of genetic algorithm, the kinematic optimization is carried out by maximizing the mean value of the local transmission index subject to the lower and upper bounds of design variables. The numerical result shows that the optimized parallel mechanism can achieve good kinematic performance in the defined task workspace.

ACKNOWLEDGEMENTS

This work is supported by the National Natural Science Foundation of China (NSFC) under grant 51405331.

REFERENCES

1. Díaz, I., Gil, J. J., and Sánchez, E., "Lower-limb robotic rehabilitation: literature review and challenges", *Journal of Robotics*, 2011.
2. Pohl, M., Werner, C., Holzgraefe, M., Kroczek, G., Wingendorf, I., Hoölig, G., Koch, R., and Hesse, S., "Repetitive locomotor training and physiotherapy improve walking and basic activities of daily living after stroke: a single-blind, randomized multicentre trial (DEutsche GAngtrainerStudie, DEGAS)", *Clinical rehabilitation*, Vol. 21, No. 1, pp. 17–27, 2007.
3. Martins, M. M., Frizera Neto, A., Santos, C., and Ceres, R., "Review and classification of human gait training and rehabilitation devices", *11th European Association for the Advancement of Assistive Technology in Europe (AAATE'11)*, 2011.
4. Colombo, G., Joerg, M., Schreier, R., and Dietz, V., "Treadmill training of paraplegic patients using a robotic orthosis", *Journal of rehabilitation research and development*, Vol. 47, No. 6, pp. 693, 2007.
5. Freivogel, S., Mehrholz, J., Husak-Sotomayor, T., and Schmalohr, D., "Gait training with the newly developed 'LokoHelp'-system is feasible for non-ambulatory patients after stroke, spinal cord and brain injury. A feasibility study", *Brain Injury*, Vol. 22, No. 7-8, pp. 625-632, 2008.
6. West, R. G., "Powered gait orthosis and method of utilizing same", US20040019304, 2004.
7. Schmidt, H., Werner, C., Bernhardt, R., Hesse, S., and Krüger, J., "Gait rehabilitation machines based on programmable footplates", *Journal of neuroengineering and rehabilitation*, Vol. 4, No. 1, pp. 1, 2007.
8. Schmidt, H., "HapticWalker-A novel haptic device for walking simulation", *Proc. of'EuroHaptics*, 2004.
9. Yano, H., Tamefusa, S., Tanaka, N., Saitou, H., and Iwata, H., "Gait rehabilitation system for stair climbing and descending", *2010 IEEE Haptics Symposium*, pp. 393-400, 2010.
10. Yoon, J., Novandy, B., Yoon, C. H., and Park, K. J., "A 6-DOF gait rehabilitation robot with upper and lower limb connections that allows walking velocity updates on various terrains", *IEEE/ASME Transactions on Mechatronics*, Vol. 15, No. 2, pp. 201-215, 2010.
11. Yoon, J., and Ryu, J., "A novel locomotion interface with two 6-dof parallel manipulators that allows human walking on various virtual terrains", *The International Journal of Robotics Research*, Vol. 25, No. 7, pp. 689-708, 2006.

12. Huang, T., Li, M., Li, Z., Chetwynd, D. G., and Whitehouse, D. J., "Optimal kinematic design of 2-DOF parallel manipulators with well-shaped workspace bounded by a specified conditioning index", *IEEE Transactions on Robotics and Automation*, Vol. 20, No. 3, pp. 538-543, 2004.
13. Chablat, D., and Wenger, P., "Architecture optimization of a 3-DOF translational parallel mechanism for machining applications, the Orthoglide", *IEEE Transactions on Robotics and Automation*, Vol. 19, No. 3, pp. 403-410, 2003.
14. Gosselin, C. M., and Angeles, J., "the optimum kinematic design of a spherical three-degree-of-freedom parallel manipulator", *Journal of mechanisms, transmissions, and automation in design*, Vol. 111, No. 2, pp. 202-207, 1989.
15. Merlet, J. P., "Jacobian, manipulability, condition number, and accuracy of parallel robots", *Journal of Mechanical Design*, Vol. 128, No. 1, pp. 199-206, 2006.
16. Angeles, J., "Is there a characteristic length of a rigid-body displacement", *Mechanism and Machine Theory*, Vol. 41, No. 8, pp. 884-896, 2006.
17. Liu, H., Huang, T., and Chetwynd, D. G., "A method to formulate a dimensionally homogeneous jacobian of parallel manipulators", *IEEE Transactions on Robotics*, Vol. 27, No. 1, pp. 150-156, 2011.
18. Ball, R. S., *A Treatise on the Theory of Screws*, Cambridge university press, 1998.
19. Freudenstein, F., and Woo, L. S. "Kinematic Analysis of Spatial Mechanisms by Means of Screw Coordinates. Part 2—Analysis of Spatial Mechanisms", *Journal of Engineering for Industry*, Vol. 93, No. 1, pp. 67-73, 1971.
20. Sutherland, G., and Roth, B., "A transmission index for spatial mechanisms", *ASME Journal of Engineering for Industry*, Vol. 95, No. 2, pp. 589-597, 1973.
21. Chen, C., and Angeles, J., "Generalized transmission index and transmission quality for spatial linkages", *Mechanism and Machine Theory*, Vol. 42, No. 9, pp. 1225-1237, 2007.
22. Liu, X. J., Wu, C., and Wang, J., "A new approach for singularity analysis and closeness measurement to singularities of parallel manipulators", *Journal of Mechanisms and Robotics*，Vol. 4, No. 4, p. 041001, 2012.
23. Liu, H., Huang, T., Kecskeméthy, A., and Chetwynd, D. G., "A generalized approach for computing the transmission index of parallel mechanisms", *Mechanism and Machine Theory*, Vol. 74, pp. 245-256, 2014.
24. Liu, X., Wu, C., and Xie, F., "Motion/force transmission indices of parallel manipulators", *Frontiers of Mechanical Engineering*, Vol. 6, No. 1, pp. 89-91, 2011.
25. Liu, H., Jia, X., Xiong, K., and Xie, S., "A parallel manipulator for ankle rehabilitation", CN105943307A, 2016.
26. CGA Normative Gait Database. Avaliable at: http://www.clinicalgaitanalysis.com
27. Huang, T., Liu, H. T., and Chetwynd, D. G., "Generalized Jacobian analysis of lower mobility manipulators," *Mechanism and Machine Theory*, Vol. 46, No. 6, pp. 831-844, 2011.
28. Dai, J. S., Huang, Z., and Lipkin, H., "Mobility of overconstrained parallel mechanisms," *Journal of Mechanical Design*, Vol. 128, No. 1, pp. 220-229, 2006.
29. Liu, H. T., Wang, M., Huang, T., Chetwynd, D. G., and Kecskeméthy, A., "A dual space approach for force/motion transmissibility analysis of lower mobility parallel manipulators," *Journal of Mechanisms and Robotics*, Vol. 7, No. 3, p. 034504, 2015.
30. Huang, T., Yang, S., Wang, M., Sun, T., and Chetwynd, D. G., "An approach to determining the unknown twist/wrench subspaces of lower mobility serial kinematic chains," *Journal of Mechanisms and Robotics*, Vol. 7, No. 3, p. 031003, 2015.
31. Gan, D., Dias, J., and Seneviratne, L., "Unified kinematics and optimal design of a 3rRPS metamorphic parallel mechanism with a reconfigurable revolute joint,", *Mechanism and Machine Theory*, Vol. 96, pp. 239-254, 2016.